

Structural and Rate Studies of the 1,2-Additions of Lithium Phenylacetylide to Lithiated Quinazolinones: Influence of Mixed Aggregates on the Reaction Mechanism

Timothy F. Briggs,[†] Mark D. Winemiller,[†] David B. Collum,^{*,†}
 Rodney L. Parsons, Jr.,[‡] Akin H. Davulcu,[‡] Gregory D. Harris,[‡]
 Joseph M. Fortunak,[‡] and Pat N. Confalone[‡]

Contribution from the Department of Chemistry and Chemical Biology, Baker Laboratory, Cornell University, Ithaca, New York 14853-1301, and Bristol Myers-Squibb Company, Process Research and Development, One Squibb Drive, New Brunswick, New Jersey 08903

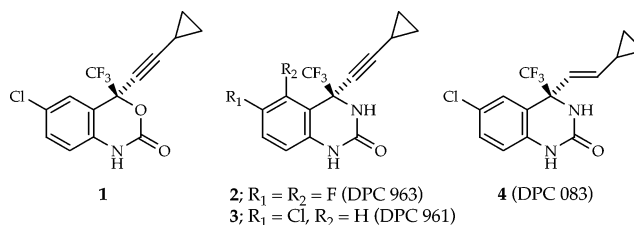
Received October 10, 2003; E-mail: dbc6@cornell.edu

Abstract: The 1,2-addition of lithium phenylacetylide (PhCCLi) to quinazolinones was investigated using a combination of structural and rate studies. ⁶Li, ¹³C, and ¹⁹F NMR spectroscopies show that deprotonation of quinazolinones and phenylacetylene in THF/pentane solutions with lithium hexamethyldisilazide affords a mixture of lithium quinazolinide/PhCCLi mixed dimer and mixed tetramer along with PhCCLi dimer. Although the mixed tetramer dominates at high mixed aggregate concentrations and low temperatures used for the structural studies, the mixed dimer is the dominant form at the low total mixed aggregate concentrations, high THF concentrations, and ambient temperatures used to investigate the 1,2-addition. Monitoring the reaction rates using ¹⁹F NMR spectroscopy revealed a first-order dependence on mixed dimer, a zeroth-order dependence on THF, and a half-order dependence on the PhCCLi concentration. The rate law is consistent with the addition of a disolvated PhCCLi monomer to the mixed dimer. Investigation of the 1,2-addition of PhCCLi to an O-protected quinazolinone implicates reaction via trisolvated PhCCLi monomers.

Introduction

Several new classes of potent nonnucleoside reverse transcriptase inhibitors have been developed by DuPont Pharmaceuticals and Merck Research Laboratories.¹ Efavirenz (**1**) is now widely prescribed under the names Sustiva and Stocrin for the treatment of AIDS and symptomatic HIV-1 infection.^{2–4} Second-generation drug candidates **2**, **3**, and **4** possess significant activity against wild-type HIV and mutant strains resistant to currently approved drug regimens,^{1,5,6} propelling them to advanced clinical trials.⁵

Reverse transcriptase inhibitors **2–4** are prepared on a large scale, up to 5000 kg, in greater than 98% enantiomeric excess



by the 1,2-addition illustrated in eq 1. This remarkable reaction presents a challenging problem in structural and mechanistic organolithium chemistry. The five lithium salts—**6**, **7**, **8**, **9**, and lithium hexamethyldisilazide (LiHMDS)—could aggregate in countless proportions, connectivities, and stereochemistries that would likely depend markedly on solvent, temperature, concentration, and stoichiometries.⁷ Previous structural studies have shown that the underlying aggregation effects are indeed very complex.^{8–11}

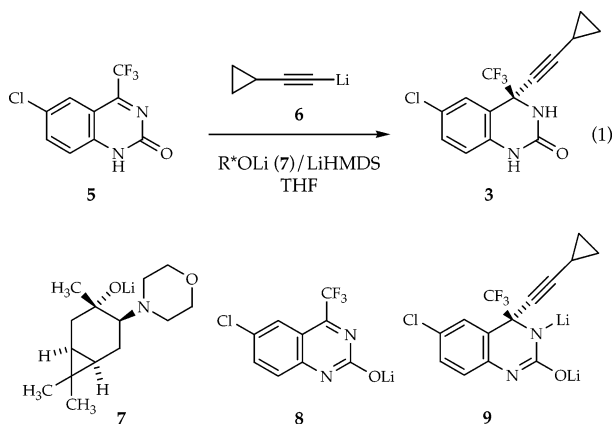
As a key step toward understanding the enantioselective 1,2-addition, we have investigated the nonenantioselective variant

[†] Cornell University.

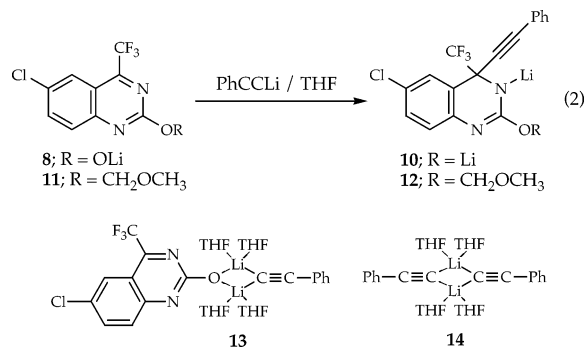
[‡] Bristol Myers-Squibb Co.

- (1) For a review of the syntheses of nonnucleoside reverse transcriptase inhibitors, see: Parsons, R. L., Jr. *Curr. Opin. Drug Discovery Dev.* **2000**, *3*, 783.
- (2) Young, S. D.; Britcher, S. F.; Tran, L. O.; Payne, L. S.; Lumma, W. C.; Lyle, T. A.; Huff, J. R.; Anderson, P. S.; Olsen, D. B.; Carroll, S. S.; Pettibone, D. J.; O'Brien, J. A.; Ball, R. G.; Balani, S. K.; Lin, J. H.; Chen, I.-W.; Schleif, W. A.; Sardana, V. V.; Long, W. J.; Byrnes, V. W.; Emini, E. A. *Antimicrob. Agents Chemother.* **1995**, *39*, 2602.
- (3) Pierce, M. E.; Parsons, R. L., Jr.; Radesca, L. A.; Lo, Y. S.; Silverman, S.; Moore, J. R.; Islam, Q.; Choudhury, A.; Fortunak, J. M.; Nguyen, D.; Luo, C.; Morgan, S. J.; Davis, W. P.; Confalone, P. N.; Chen, C. Y.; Tillyer, R. D.; Frey, L.; Tan, L.; Xu, F.; Zhao, D. L.; Thompson, A. S.; Corley, E. G.; Grabowski, E. J. J.; Reamer, R.; Reider, P. J. *J. Org. Chem.* **1998**, *63*, 8536. Thompson, A. S.; Corley, E. G.; Huntington, M. F.; Grabowski, E. J. *J. Tetrahedron Lett.* **1995**, *36*, 8937.
- (4) Efavirenz is currently prepared by an amino alcohol-mediated addition of alkynyl zinc derivatives. Tan, L.; Chen, C. Y.; Tillyer, R. D.; Grabowski, E. J. J.; Reider, P. J. *Angew. Chem., Int. Ed.* **1999**, *38*, 711. Chen, C. Y.; Tan, L. *Enantiomer* **1999**, *4*, 599.

- (5) Tucker, T. J.; Lyle, T. A.; Wiscourt, C. M.; Britcher, S. F.; Young, S. D.; Sanders, W. M.; Lumma, W. C.; Goldman, M. E.; O'Brien, J. A.; Ball, R. G.; Homnick, C. F.; Schleif, W. A.; Emini, E. A.; Huff, J. R.; Anderson, P. S. *J. Med. Chem.* **1994**, *37*, 2437. Corbett, J. W.; Ko, S. S.; Rodgers, J. D.; Gearhart, L. A.; Magnus, N. A.; Bachelier, L. T.; Diamond, S.; Jeffrey, S.; Klabe, R. M.; Cordova, B. C.; Garber, S.; Logue, K.; Trainor, G. L.; Anderson, P. S.; Erickson-Viitanen, S. K. *Antimicrob. Agents Chemother.* **1999**, *43*, 2893.
- (6) Kauffman, G. S.; Harris, G. D.; Dorow, R. L.; Stone, B. R. P.; Parsons, R. L., Jr.; Pesti, J. A.; Magnus, N. A.; Fortunak, J. M.; Confalone, P. N.; Nugent, W. A. *Org. Lett.* **2000**, *2*, 3119.



in eq 2. Several simplifications in the protocol have provided sufficient control over aggregate structures to allow detailed rate studies. We preface the mechanistic study by foreshadowing results from the structural studies: Treating THF solutions of quinazolinone **5** and phenylacetylene with LiHMDS under judiciously chosen conditions affords mixed dimer **13** and lithium phenylacetylide (PhCCLi) dimer **14** as the predominant species. The most central and pressing question is what role does mixed dimer **13** play in the 1,2-addition? At the outset, we considered two plausible answers: (1) mixed dimer **13** reacts via an intramolecular mechanism that exploits the reagent proximities afforded by mixed aggregation, or (2) mixed dimer **13** is simply a protected form of quinazolinone **5** that undergoes 1,2-addition by an external nucleophilic PhCCLi fragment.¹² A comparison with rate studies of the 1,2-addition to O-protected quinazolinone derivative **11** (eq 2) reveals notable similarities and differences.



Results

Structural Studies. A combination of forethought and serendipity allowed us to control the organolithium solution

- (7) For leading references to structural studies of RLi/R'OLi mixed aggregates, see: Thomas, R. D.; Huang, H. *J. Am. Chem. Soc.* **1999**, *121*, 1, 11239. Lochmann, L. *Eur. J. Inorg. Chem.* **2000**, 1115. Sorger, K.; Schleyer, P. v. R.; Fleischer, R.; Stalke, D. *J. Am. Chem. Soc.* **1996**, *118*, 6924. Jackman, L. M.; Rakiewicz, E. F. *J. Am. Chem. Soc.* **1991**, *113*, 1202. Kremer, T.; Harder, S.; Junge, M.; Schleyer, P. v. R. *Organometallics* **1996**, *15*, 585.
- (8) (a) Thompson, A.; Corley, E. G.; Huntington, M. F.; Grabowski, E. J. J.; Remenar, J. F.; Collum, D. B. *J. Am. Chem. Soc.* **1998**, *120*, 2028. (b) Xu, F.; Reamer, R. A.; Tillyer, R.; Cummins, J. M.; Grabowski, E. J. J.; Reider, P. J.; Collum, D. B.; Huffman, J. C. *J. Am. Chem. Soc.* **2000**, *122*, 11212.
- (9) (a) Parsons, R. L., Jr.; Fortunak, J. M.; Dorow, R. L.; Harris, G. D.; Kauffman, G. S.; Nugent, W. A.; Winemiller, M. D.; Briggs, T. F.; Xiang, B.; Collum, D. B. *J. Am. Chem. Soc.* **2001**, *123*, 9135. (b) Briggs, T. F.; Winemiller, M. D.; Xiang, B.; Collum, D. B. *J. Org. Chem.* **2001**, *66*, 6291. (c) Sun, X.; Winemiller, M. D.; Xiang, B.; Collum, D. B. *J. Am. Chem. Soc.* **2001**, *123*, 8039.
- (10) The asymmetric additions are based on work by Jackman and co-workers: Ye, M.; Logaraj, S.; Jackman, L. M.; Hillegass, K.; Hirsh, K. A.; Bollinger, A. M.; Grosz, A. L.; Mani, V. *Tetrahedron* **1994**, *50*, 6109.
- (11) Briggs, T. F.; Winemiller, M. D.; Collum, D. B., unpublished.

Table 1. ⁶Li, ¹³C, and ¹⁹F NMR Spectroscopic Data^a

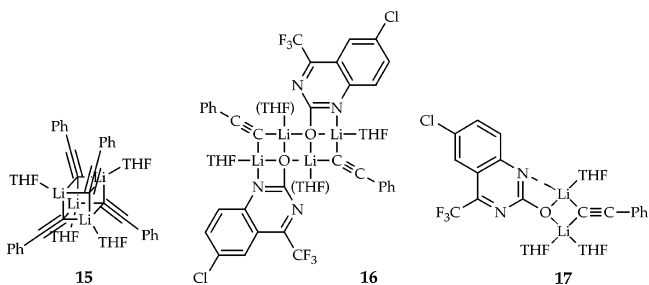
compd	δ ⁶ Li (m, J_{Li-C} ; m, J_{Li-N}) ^b	δ ¹³ C (m, J_{Li-C})	δ ¹⁹ F
8	2.25 (–; d, 2.5 Hz) 1.04 (–; s) 0.80 (–; s)		–64.7, –65.2
10	– ^c		–80.6 to –80.3 (br mound)
13	0.59 (d, 8.5 Hz; s)	139.07 (qn, 8.6 Hz)	–64.8
14	0.48 (t, 8.4 Hz; –)	139.35 (qn, 8.4 Hz)	–
16	1.75 (d, 9.0 Hz; d, 3.6 Hz) 0.77 (d, 8.1 Hz; s)	137.54 (qn, 8.5 Hz)	–65.1

^a The J_{C-Li} coupling constants were measured from the $1J(^6Li, ^{13}C)$ -resolved spectrum. The multiplicities are denoted as follows: s = singlet, d = doublet, t = triplet, qn = quintet. The ⁶Li, ¹³C, and ¹⁹F chemical shifts are reported relative to 0.3 M ⁶LiCl/MeOH at –90 °C (δ ⁶Li = 0.0 ppm), hexafluorobenzene at –110 °C (δ ¹⁹F = –162.55 ppm), and the CH₂O carbon of THF at –115 °C (δ ¹³C = 67.97 ppm), respectively. All J values are reported in hertz. ^b The indicated ⁶Li–¹⁵N coupling is only observed using [1-¹⁵N]**5**. ^c Complex envelope of peaks between 0 and 2 ppm.

structures sufficiently to carry out detailed mechanistic studies. The results from NMR spectroscopic studies are summarized in Table 1 and are described below. Selected spectra are illustrated in Figures 1 and 2.

LiHMDS is readily purified through recrystallization,¹³ serves as an excellent proton scavenger,⁹ and does not form mixed aggregates except under unusual conditions.^{9,14,15} Indeed, a mixture of PhCCLi and lithium salt **8** generated in situ with excess [⁶Li]LiHMDS¹³ contains no LiHMDS-derived mixed aggregates.

PhCCLi proves especially important to the success of the solution kinetics. Lithium cyclopropylacetylide (**6**) and other lithium acetylides typically exist as mixtures of cyclic dimers and cubic tetramers in THF and THF/hydrocarbon solutions.^{8,9,16–18} Lithium phenylacetylide in THF/toluene shows a greater tendency to form dimer **14** than do most lithium acetylides, but it affords tetramer **15** at low THF concentrations.¹⁸ Such a dimer–tetramer mixture would undermine the rate studies. In contrast, ⁶Li and ¹³C NMR spectra recorded on THF/pentane mixtures of [⁶Li, ¹³C]PhCCLi reveal exclusively dimer **14** (Table 1) in solutions containing as little as 20% THF by volume. The pronounced hydrocarbon effect can be witnessed by incrementally replacing the toluene in 20% THF/toluene solutions of PhCCLi with pentane, causing conversion of a 2:1 **15**:**14** mixture to exclusively dimer **14**. The origins of this odd hydrocarbon dependence are being investigated.¹⁸ As a practical matter, THF/pentane mixtures offer important structural control for the rate studies.



In situ generation of quinazolinone salt **8** in THF or THF/pentane affords a complex mixture that is characteristic of N-lithiated carboxamides in the absence of added lithium salts.^{11,19,20} In the presence of excess [⁶Li, ¹³C]PhCCLi, however, we observe two species displaying spectral data consistent with

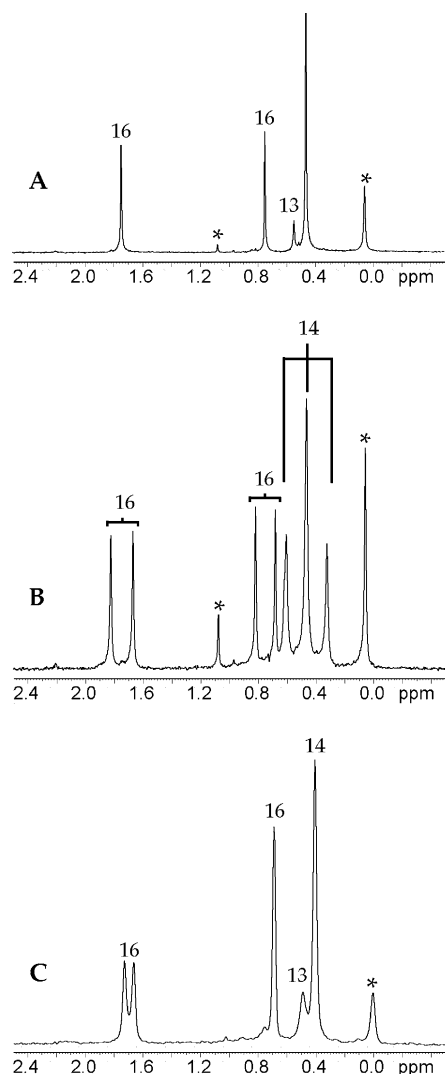


Figure 1. ^6Li spectra were recorded at $-115\text{ }^\circ\text{C}$. Spectra A and B were recorded on a 2:1 mixture of $[\text{}^6\text{Li},^{13}\text{C}]\text{PhCCLi}$ (0.133 N) and $[\text{}^6\text{Li}]\mathbf{8}$ (0.067 N) in 7.6 M THF/pentane; spectrum C was recorded on a 2:1 mixture of $[\text{}^6\text{Li}]\text{PhCCLi}$ (0.20 N) and $[\text{}^6\text{Li},1\text{-}^{15}\text{N}]\mathbf{8}$ (0.10 N) in 9.5 M THF/pentane. (Residual $[\text{}^6\text{Li}]\text{LiHMDS}$ is marked by *). Spectrum A is ^{13}C broad-band decoupled.

mixed dimer **13** and mixed tetramer **16** (Figure 1; Table 1). A 5-fold excess of PhCCLi is required to convert quinazolinone salt **8** completely to the mixed aggregates.

Mixed dimer **13** displays a ^6Li doublet due to coupling to a single ^{13}C nucleus that is readily discerned from the other

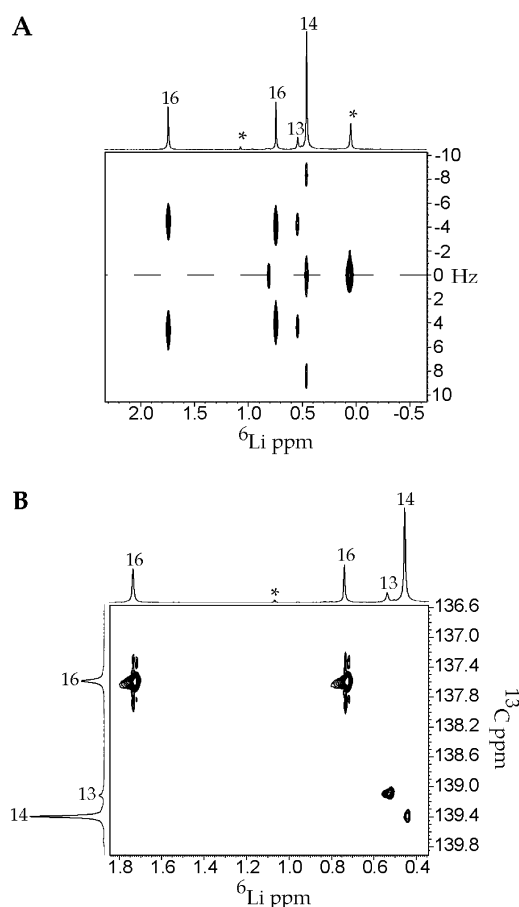


Figure 2. $J(^6\text{Li},^{13}\text{C})$ -resolved spectrum (A) and $^6\text{Li},^{13}\text{C}$ -HMQC spectrum (B) recorded on 0.133 N $[\text{}^6\text{Li},^{13}\text{C}]\text{PhCCLi}$ and 0.067 N $[\text{}^6\text{Li}]\mathbf{8}$ in 7.6 M THF (pentane cosolvent) at $-115\text{ }^\circ\text{C}$. $[\text{}^6\text{Li}]\text{LiHMDS}$ is indicated by an asterisk (*).

multipeaks in the $J(^6\text{Li},^{13}\text{C})$ -resolved⁹ and $^6\text{Li},^{13}\text{C}$ -heteronuclear multiple quantum coherence (HMQC)^{21,22} spectra (Figure 2).²³ A ^{13}C quintet indicates coupling to two symmetry-equivalent lithium nuclei. The lack of chelation by the quinazolinone is confirmed by the absence of coupling when dimer **13** is generated from ^{15}N -enriched quinazolinones $[1\text{-}^{15}\text{N}]\mathbf{5}$ and $[3\text{-}^{15}\text{N}]\mathbf{5}$. A single ^{19}F resonance attests to the symmetry of mixed dimer **13** and provides a means to monitor reaction rates (vide infra).

Mixed tetramer **16** manifests two lithium resonances in a 1:1 ratio (Figure 1A). Both ^6Li resonances are coupled to a common

- (12) Carboxamides are often protected as their N-lithiated forms. For several representative examples, see: Kelly, T. R.; Lebedev, R. L. *J. Org. Chem.* **2002**, *67*, 2197. Basu, A.; Thayumanavan, S. *Angew. Chem., Int. Ed.* **2002**, *41*, 716.
- (13) Romesberg, F. E.; Bernstein, M. P.; Gilchrist, J. H.; Harrison, A. T.; Fuller, D. J.; Collum, D. B. *J. Am. Chem. Soc.* **1993**, *115*, 3475.
- (14) (a) Lucht, B. L.; Collum, D. B. *Acc. Chem. Res.* **1999**, *32*, 1035. (b) Romesberg, F. E.; Collum, D. B. *J. Am. Chem. Soc.* **1994**, *116*, 9198.
- (15) LiHMDS forms mixed aggregates with (a) hindered lithium enolates in THF solution: Kim, Y.-J.; Streitwieser, A. *Org. Lett.* **2002**, *4*, 573. (b) In the presence of poorly coordinating solvents: Zhao, P.; Collum, D. B. *J. Am. Chem. Soc.* **2003**, *125*, in press. (c) Ester enolates bearing a β -amino group.
- (16) Lithium acetylide solution structural studies: (a) Fraenkel, G.; Stier, M. *Prepr. Pap.-Am. Chem. Soc., Div. Fuel Chem.* **1985**, *30*, 586. (b) Fraenkel, G.; Pramanik, P. *J. Chem. Soc., Chem. Commun.* **1983**, 1527. (c) Gareyev, R.; Streitwieser, A. *J. Org. Chem.* **1996**, *61*, 1742. (d) Goraliski, P.; Legoff, D.; Chabanel, M. *J. Organomet. Chem.* **1993**, *456*, 1.
- (17) (a) Hässig, v. R.; Seebach, D. *Helv. Chim. Acta* **1983**, *66*, 2269. (b) Bauer, W.; Seebach, D. *Helv. Chim. Acta* **1984**, *67*, 1972. (c) Jackman, L. M.; Scarmoutzos, L. M.; DeBrosse, C. W. *J. Am. Chem. Soc.* **1987**, *109*, 5355.

- (18) Breslin, S. R.; Collum, D. B., unpublished.
- (19) Gallagher, D. J.; Du, H.; Long, S. A.; Beak, P. *J. Am. Chem. Soc.* **1996**, *118*, 11391. Maetzke, T.; Hidber, C. P.; Seebach, D. *J. Am. Chem. Soc.* **1990**, *112*, 8248. Maetzke, T.; Seebach, D. *Organometallics* **1990**, *9*, 3032. Chivers, T.; Downard, A.; Yap, G. P. A. *Inorg. Chem.* **1998**, *37*, 5708. Liddle, S. T.; Clegg, W. *Chem. Commun.* **2001**, *17*, 1584. Liddle, S. T.; Clegg, W. *J. Chem. Soc., Dalton Trans.* **2002**, *21*, 3293. Boss, S. R.; Haigh, R.; Linton, D. J.; Schooler, P.; Shield, G. P.; Wheatley, A. E. *J. Chem. Soc., Dalton Trans.* **2003**, *5*, 1001.
- (20) N-Lithiated carboxamides form mixed aggregates with lithium acetylides as well as lithium alkoxides (such as **7**): Winemiller, M. D.; Collum, D. B., unpublished.
- (21) Xiang, B.; Winemiller, M. D.; Briggs, T. F.; Fuller, D. J.; Collum, D. B. *Magn. Reson. Chem.* **2001**, *39*, 137.
- (22) (a) Günther, H.; Moskau, D.; Bast, P.; Schmalz, D. *Angew. Chem., Int. Ed. Engl.* **1987**, *26*, 1212. (b) Braun, S.; Kalinowski, H. O.; Berger, S. *150 and More Basic NMR Experiments*, 2nd ed.; Wiley-VCH: New York, 1998; p 350.
- (23) Günther, H. *J. Braz. Chem.* **1999**, *10*, 241. Mons, H.-E.; Günther, H.; Maercker, A. *Chem. Ber.* **1993**, *126*, 2747. Günther, H. In *Advanced Applications of NMR to Organometallic Chemistry*; Gielen, M., Willem, R., Wrackmeyer, B., Eds.; Wiley & Sons: Chichester, 1996; Chapter 9.

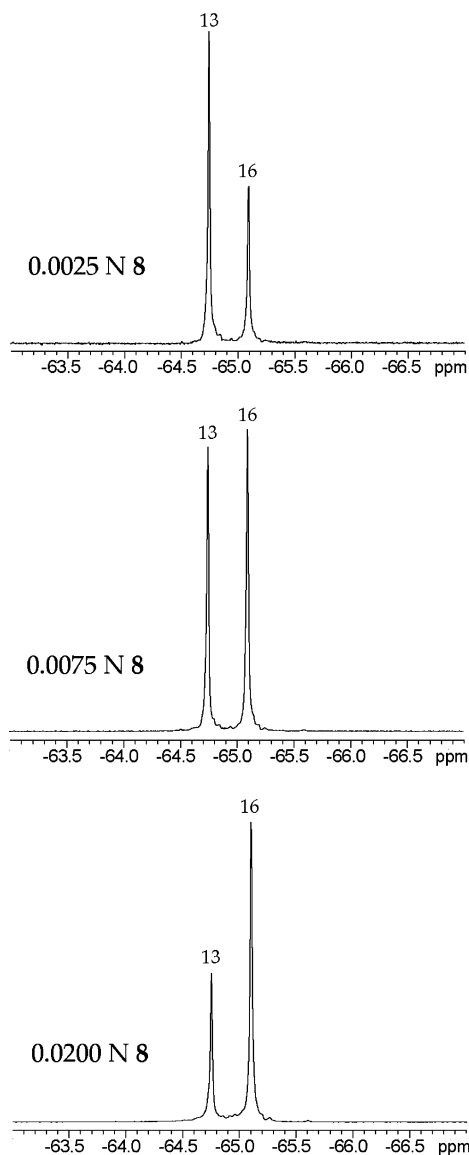
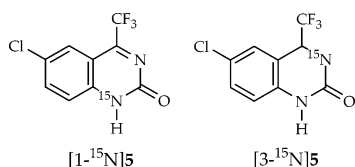


Figure 3. ^{19}F NMR spectra recorded at $-100\text{ }^\circ\text{C}$ of 7.6 M THF/pentane solutions of 0.10 N PhCCl_2 and **8** (at the normality indicated).

^{13}C nucleus (Figure 1B and 2B). Tetramer **16** prepared from $[1\text{-}^{15}\text{N}]\mathbf{5}$ shows a distinct N–Li coupling in one ^6Li resonance (Figure 1C), whereas **16** prepared from $[3\text{-}^{15}\text{N}]\mathbf{5}$ affords no coupling. Several isomers of tetramer **16** are consistent with the spectroscopic data.²⁴ Cubic tetramers, however, are excluded by the coupling patterns.^{8,9}



We originally suspected the chelated mixed oligomer to be mixed dimer **17** rather than mixed tetramer **16**. The spectroscopically opaque O–Li linkages render **16** and **17** difficult to distinguish. However, the chelated form is promoted relative to mixed dimer **13** at elevated total mixed aggregate concentrations (Figure 3) and low THF concentrations (Figure 4), suggesting the chelated form has a lower solvation number and higher aggregation state than those of mixed dimer **13**.

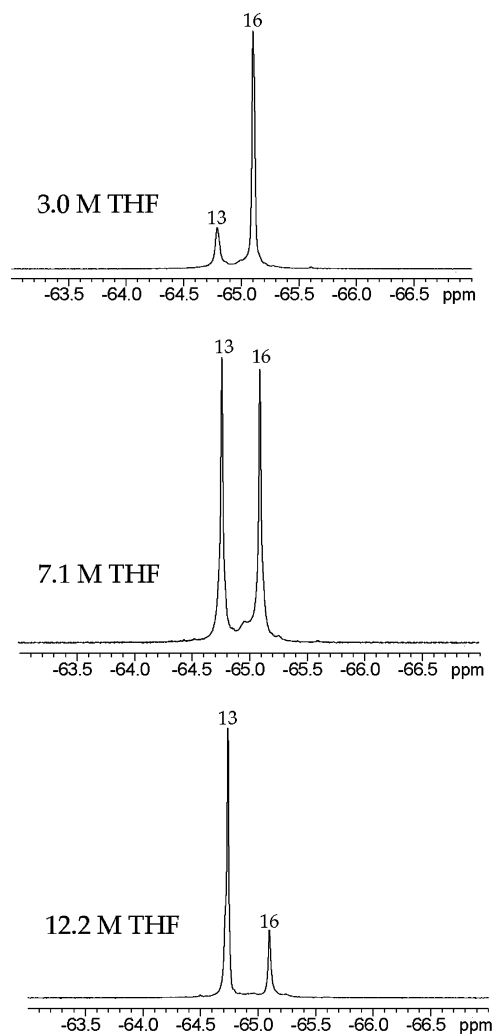


Figure 4. ^{19}F NMR spectra recorded at $-80\text{ }^\circ\text{C}$ of THF/pentane solutions of 0.04 N PhCCl_2 and 0.01 N **8** at the THF concentrations indicated.

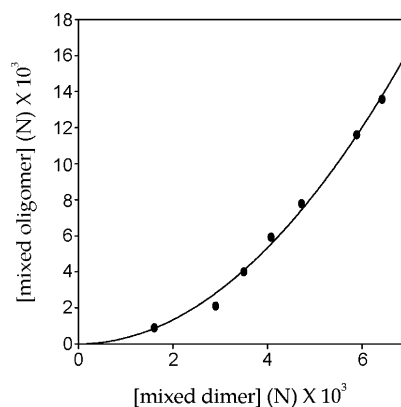


Figure 5. Plot of [mixed dimer] versus [mixed oligomer] (measured in normality of subunit **8**) in 8.0 M THF solutions containing 0.10 N PhCCl_2 and a range of concentrations of **8** in pentane cosolvent at $-100\text{ }^\circ\text{C}$. The curve depicts an unweighted least-squares fit to $[\text{mixed oligomer}] = K' [\text{mixed dimer}]^m$ ($K' = (3 \pm 2) \times 10^2$, $m = 2.0 \pm 0.1$).

The relationship of the chelated form to mixed dimer **13** is described according to eqs 3 and 4, which can be rearranged to eq 5. Keeping THF at a high fixed concentration, plotting the relative concentrations of the mixed aggregates (Figure 5) enables calculation of a relative aggregation number, $m = 2.0 \pm 0.1$, that is consistent with the mixed tetramer assignment.

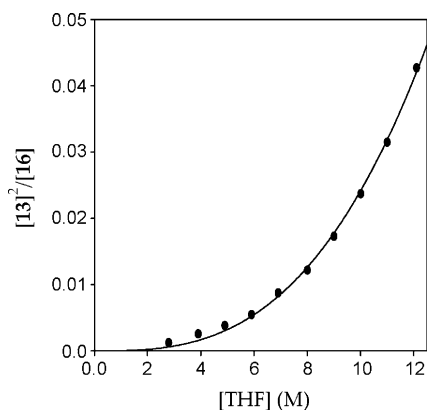
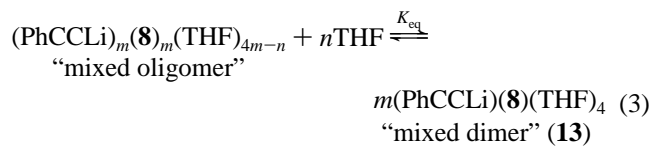


Figure 6. Plot of [mixed dimer]²/[mixed tetramer] (i.e., [13]²/[16]) versus [THF] of solutions containing 0.04 N PhCCLi and 0.01 N **8** over a range of THF concentrations in pentane cosolvent at $-80\text{ }^{\circ}\text{C}$. The curve depicts an unweighted least-squares fit to $[\mathbf{13}]^2/[\mathbf{16}] = K_{\text{eq}}[\text{THF}]^n$ ($K_{\text{eq}} = (3.0 \pm 0.5) \times 10^{-5}$, $n = 2.91 \pm 0.07$).

In turn, maintaining a fixed concentration of mixed aggregate and varying the THF concentration (eq 6, Figure 6) affords a high relative per-lithium solvation number, $n = 2.91 \pm 0.07$. Although the measured solvation number seems to implicate an unsymmetrically solvated tetramer,²⁵ a systemic error causing a deviation from an integer value of either 2.0 or 4.0 seems equally plausible.



$$K_{\text{eq}} = [\text{mixed dimer}]^m / \{[\text{THF}]^n [\text{mixed oligomer}]\} \quad (4)$$

$$[\text{mixed oligomer}] = K'[\text{mixed dimer}]^m \quad (5)$$

$$K' = 1/K_{\text{eq}}[\text{THF}]^n \approx \text{constant}$$

$$[\text{mixed dimer}]^m / [\text{mixed oligomer}] = K_{\text{eq}}[\text{THF}]^n \quad (6) \quad (m = 2 \text{ from Figure 5})$$

Although the complexity caused by the pair of mixed aggregates did not bode well for detailed rate studies, we observed a somewhat surprising and fortuitous promotion of dimer **13** relative to tetramer **16** (Figure 7) at elevated temperatures. Indeed, monitoring the temperature-dependent **13/16** ratios in six combinations of THF and mixed aggregate concentrations (Figure 8 is emblematic) affords relatively invariant (concentration-independent) thermodynamic parameters: $\Delta H^\circ = 1.8 \pm 0.1$ kcal/mol and $\Delta S^\circ = -11.6 \pm 0.9$ cal/(mol·K).²⁶ Figure 9 shows a plot of the calculated mole fraction of dimer **13** as a function of THF under conditions that are representative of those used in the rate studies. Thus, under

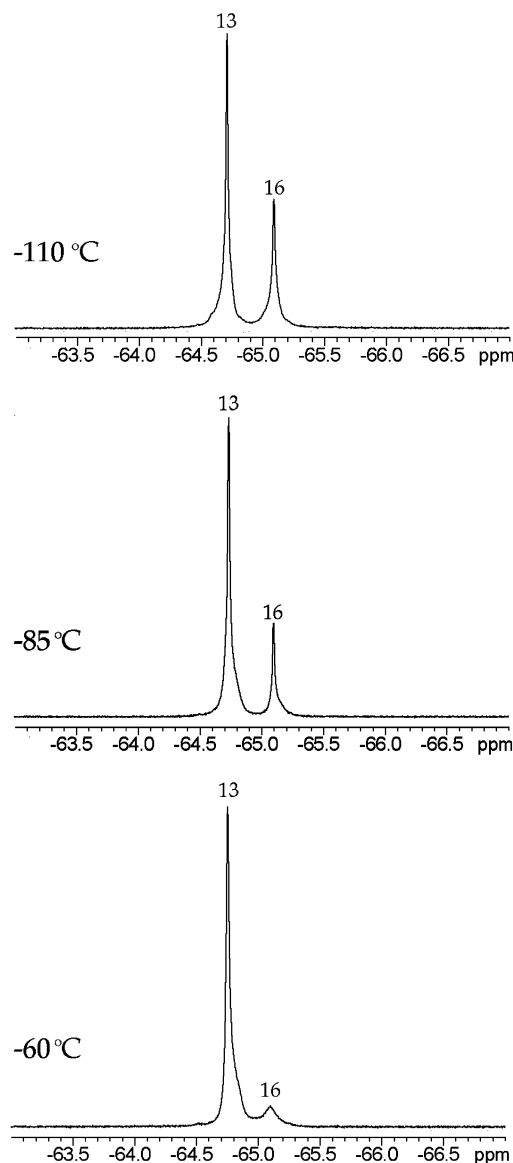


Figure 7. ¹⁹F NMR spectra recorded on a neat THF solution of 0.10 N PhCCLi and 0.005 N **8** at the temperatures indicated.

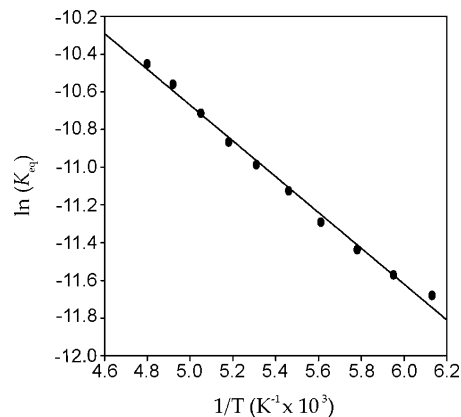


Figure 8. Plot of $\ln(K_{\text{eq}})$ versus $(1/T)$ of a solution containing 0.10 N PhCCLi and 0.005 N **8** in neat THF. The curve depicts an unweighted least-squares fit to $\ln(K_{\text{eq}}) = (-\Delta H/R)(1/T) + \Delta S/R$ ($\Delta H = 1.89 \pm 0.05$ kcal/mol, $\Delta S = -11.7 \pm 0.2$ cal/(mol·K)).

carefully controlled conditions, dimer **13** is dominant, and tetramer **16** is largely irrelevant to the rate studies (vide infra).

- (24) Organolithium ladder structures: Gregory, K.; Schleyer, P. v. R.; Snaith, R. *Adv. Inorg. Chem.* **1991**, *37*, 47. Mulvey, R. E. *Chem. Soc. Rev.* **1991**, *20*, 167. Beswick, M. A.; Wright, D. S. In *Comprehensive Organometallic Chemistry II*; Abel, E. W., Stone, F. G. A., Wilkinson, G., Eds.; Pergamon: New York, 1995; Vol. 1, Chapter 1. Mulvey, R. E. *Chem. Soc. Rev.* **1998**, *27*, 339 and references cited within.
- (25) For examples of lithium aggregates displaying a noninteger per-lithium solvation number, see: Seebach, D.; Bauer, W.; Hansen, J.; Laube, T.; Schweizer, W. B.; Dunitz, J. D. *J. Chem. Soc., Chem. Commun.* **1984**, 853. Depue, J. S.; Collum, D. B. *J. Am. Chem. Soc.* **1988**, *110*, 5518.
- (26) The ¹⁹F resonances of **13** and **16** coalesce at $-55\text{ }^{\circ}\text{C}$.

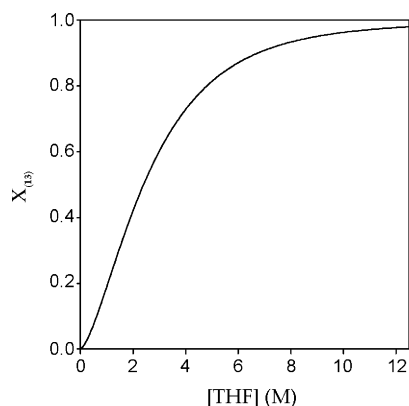


Figure 9. Plot of the mole fraction of **13** (X_{13}) versus THF concentration (M) for a solution of **13** and **16** at 10 °C (total normality = 0.005 N). The curve was constructed from the experimentally determined values of $K_{eq} = 1.20 \times 10^{-4}$, $m = 2$, and $n = 3$ (see eqs 3–6) and a complex expression derived in the Supporting Information.

The temperature- and concentration-dependent dimer–tetramer equilibrium requires additional comment. Conventional wisdom suggests that the more highly solvated lower aggregate would be favored at low temperatures due to a net enthalpic stabilization attributed to the stabilizing enthalpy of solvation.²⁷ In contrast, the more highly solvated dimer **13** is enthalpically and entropically disfavored when compared to tetramer **16**. The dominance of dimer **13** under the conditions used to follow the reaction rates stems from the substantial deviation from the unit-molarity standard state due to the high THF concentration and low mixed aggregate concentration.

The product of the 1,2-addition is depicted generically as dianion **10**; spectroscopic studies suggest that **10** is a mixture of species as shown by a broad mound of ^{19}F resonances. The dianion formulation (rather than a monoanion resulting from protonation by residual hexamethyldisilazane) is supported by control experiments showing that deprotonations of **2** with 1.0 and 2.0 equiv of LiHMDS afford spectroscopically distinct product distributions. Most importantly, however, the product of the reaction is of no consequence under pseudo-first-order conditions used to study the kinetics.

It is also noteworthy that the formation of **10** in the presence of excess $[\text{}^6\text{Li}]\text{PhCClLi}$ shows no evidence of PhCClLi-containing mixed aggregates. Thus, the 1,2-addition in eq 2 does not result in the net consumption of free PhCClLi dimer **14**. Consequently, conversion-dependent changes in mechanism that can dramatically increase the mechanistic complexity under stoichiometric conditions are unlikely to intervene.

Rate Studies: 1,2-Addition to Mixed Dimer 13. Pseudo-first-order conditions were established by maintaining low mixed aggregate concentrations (0.005 N), high PhCClLi concentrations, high THF concentrations (using pentane as the cosolvent), and LiHMDS in a fixed (0.10 M) excess. Under these conditions, dimer **13** is the dominant mixed aggregate, and tetramer **16** is insignificant (Figure 9). The rates of the 1,2-addition in eq 2 were initially investigated by monitoring the loss of mixed dimer **13** (1552 cm^{-1}) using in situ IR spectroscopy.²⁸ (The IR-derived rate data are archived in the Supporting Information.)

(27) Deaggregation is normally promoted at low temperatures and is widely believed to be the result of the dominance of the enthalpy affiliated with higher solvation numbers. It is unclear why the less highly solvated tetramer **16** (as shown by THF concentration dependencies) is enthalpically preferred (as shown by the temperature dependencies).

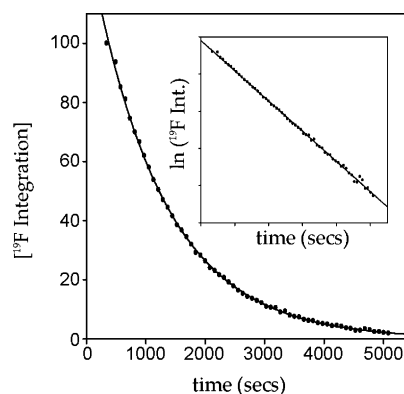


Figure 10. Plot of the ^{19}F integration versus time for the 1,2-addition of PhCClLi (0.50 N) to **13** (0.005 M) at 10 °C in a 7.75 M THF/pentane. The curve depicts an unweighted least-squares fit to $\text{integration} = \text{integration}_0 e^{-k_{\text{obsd}} t} + c$ ($k_{\text{obsd}} = (8.19 \pm 0.07) \times 10^{-4}$; $\text{integration}_0 = 136.1 \pm 0.7$; $c = 0.0 \pm 0.2$). The inset depicts the $\ln(\text{integration})$ versus time.

Unfortunately, the absorbance of **13** is obscured by a product-derived absorbance at $1505\text{--}1545\text{ cm}^{-1}$ that becomes prominent at high THF concentrations.

^{19}F NMR spectroscopy proves to be a superior analytical method for the current case study.²⁹ Monitoring the ^{19}F resonance of **13** reveals a clean first-order decay (Figure 10), provided the THF concentrations are elevated (>7.0 M in pentane). It is normal that a visually clean first-order decay in conjunction with concentration-independent values of k_{obsd} is adequate to demonstrate a first-order dependence on the limiting reagent. However, this complex case demanded that we determine the order by a best-fit protocol.³⁰ We prefer a method based on a nonlinear least-squares fit to the function in eq 7.³¹ The adjustable parameter α corresponds to the reaction order in **13**. The data for the 18 runs used to construct Figure 11 (discussed below) were fit to eq 7 and averaged, affording $\alpha = 1.05 \pm 0.03$.

$$[\mathbf{13}] = \{(\alpha - 1)k_{\text{obsd}}t + [\mathbf{13}]_0^{-(1-\alpha)}\}^{-1/(\alpha-1)} \quad (7)$$

The first-order dependence on the concentration of **13** at high THF concentration is unequivocal. At lower THF concentrations, however, tetramer **16** becomes significant (Figure 9), and we observe considerable deviations from clean first-order behavior.³² Curiously, the deviations are positive ($\alpha > 1.0$) rather than negative ($\alpha < 1.0$). (The order for a mixed-dimer based reaction would approach $\alpha = 0.5$ in the limit of complete tetramer formation.) It is possible that a new pathway intervenes at low THF concentration, but we are currently unable to provide additional insight.

The question of whether **13** reacts directly as a mixed aggregate or through the intervention of additional PhCClLi is

- (28) (a) Sun, X.; Collum, D. B. *J. Am. Chem. Soc.* **2000**, *122*, 2452. (b) Rein, A. J.; Donahue, S. M.; Pavlosky, M. A. *Curr. Opin. Drug Discovery Dev.* **2000**, *3*, 734.
- (29) For a review of structural studies using ^{19}F NMR spectroscopy, see: Gakh, Y. G.; Gakh, A. A.; Gronenborn, A. M. *Magn. Reson. Chem.* **2000**, *38*, 551.
- (30) Espenson, J. H. *Chemical Kinetics and Reaction Mechanisms*; McGraw-Hill: New York, 1995; p 31.
- (31) (a) Equation 7 is a nonlinear variant of the Noyes equation.^{31b} A derivation is found in the Supporting Information. (b) Casado, J.; Lopez-Quintela, M. A.; Lorenzo-Barral, F. M. *J. Chem. Educ.* **1986**, *63*, 450.
- (32) The deviation from a first-order fit appears as a poor fit in a plot of $[\mathbf{13}]$ versus time when fit to the function $[\mathbf{13}] = [\mathbf{13}]_0 e^{-kt}$. Fitting the data to eq 7 affords reaction orders in **13** as high as 1.4. The deviation is most easily visualized as an upward curvature in the plot of $\ln[\mathbf{13}]$ versus time (Supporting Information).

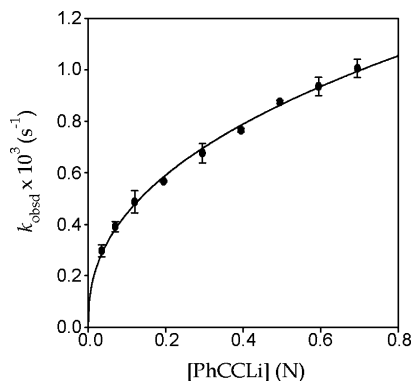


Figure 11. Plot of k_{obsd} versus [PhCCLi] in 7.75 M THF/pentane for the 1,2-addition of PhCCLi to mixed dimer **13** (0.005 N of **8**) at 10 °C. The curve depicts an unweighted least-squares fit to $k_{\text{obsd}} = a[\text{PhCCLi}]^b$ ($a = (1.16 \pm 0.01) \times 10^{-3}$, $b = 0.42 \pm 0.01$).

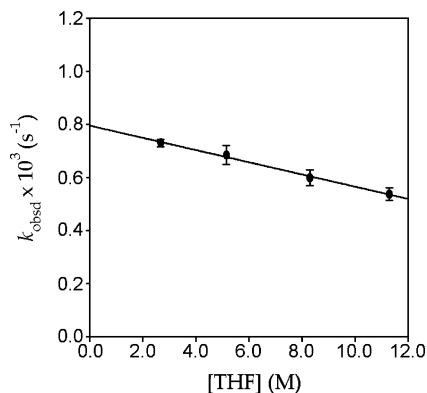


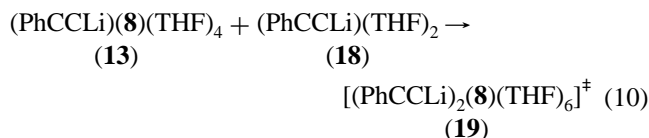
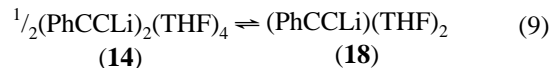
Figure 12. Plot of k_{obsd} versus [THF] in pentane cosolvent for the 1,2-addition of PhCCLi (0.20 N) to **13** (0.005 N of **8**) at 10 °C. The curve depicts an unweighted least-squares fit to $k_{\text{obsd}} = k[\text{THF}] + k'$ ($k = (-2.29 \pm 0.02) \times 10^{-5}$, $k' = (8.0 \pm 0.1) \times 10^{-4}$).

addressed by determining the rate dependencies on the PhCCLi concentration. A plot of k_{obsd} versus [PhCCLi]³³ at 7.75 M THF/pentane affords an order of 0.42 ± 0.01 (Figure 11). Although 0.42 is lower than expected,³⁴ it is strongly suggestive of the half-order dependence anticipated for a mechanism requiring deaggregation of PhCCLi dimer **14**.

A plot of k_{obsd} versus THF concentration (Figure 12) reveals nearly [THF]-independent rates.³⁵ (Recall that the values of k_{obsd} are only approximate because of deviations from a first-order decay that are due to the appearance of tetramer **16**.) The slight negative drift does not approach the >4-fold changes in k_{obsd} expected for first-order or inverse-first-order dependencies on the THF concentration. Therefore, we conclude that the predominant pathway displays a zeroth-order THF concentration dependence.

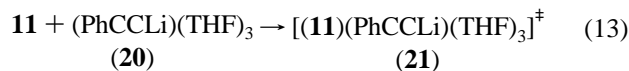
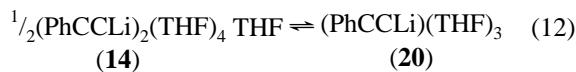
Overall, the evidence supports a first-order dependence on mixed dimer **13**, a half-order dependence on PhCCLi dimer **14**, and a zeroth-order dependence on the THF concentration. The

idealized rate law described by eq 8 is consistent with the mechanism depicted generically in eqs 9 and 10. We do not intend to suggest the requisite intermediacy of a discrete disolvated monomer **18** or even a specific sequence of events; rather, we emphasize the incorporation of the PhCCLi(THF)₂ fragment in rate-limiting transition structure **19**.



Rate Studies: 1,2-Addition to Quinazoline 11. For comparison, we monitored the 1,2-addition to O-protected quinazolinone **11**. The choice of the methoxymethyl protecting group was based on ease of synthesis and purification.³⁶ We hasten to add that there is compelling data suggesting the second oxygen linkage of the ketal can inductively influence reactivities, but the evidence also reveals that ketals do not function as polydentate ligands.^{37,38}

The 1,2-additions to **11** were carried out using methods similar to those described for the additions to **13**. Monitoring the ¹⁹F resonance of **11** shows a clean first-order decay (Supporting Information).^{39,40} The addition of PhCCLi to **11** is 10²–10³ times faster than its addition to **13**, consistent with the higher electron density on **13**. The rate data for 1,2-addition to **11** reveal notable similarities and differences with **13**. A plot of k_{obsd} versus [THF] for the addition to **11** displays a first-order dependence on the THF concentration (Figure 13). A plot of k_{obsd} versus PhCCLi concentration in 8.6 M THF reveals a fractional (0.45 ± 0.04) order. The idealized rate law (eq 11) implicates a mechanism based on trisolvated PhCCLi monomers (eqs 12 and 13).



Discussion

The highly enantioselective addition of lithium acetylides to quinazolinones illustrated in eq 1 is the key step in the syntheses

(33) The concentration of PhCCLi refers to the concentration of the monomer unit in units of normality (N).

(34) A low basal reactivity of **13** without intervention of additional lithium acetylide could explain the reduced fractional order in PhCCLi. Indeed, if the rate data are fit to $k_{\text{obsd}} = a[\mathbf{13}]^b + c$, a small nonzero intercept, c , is accompanied by a fractional order of $b = 0.54$. We hasten to add, however, that such fits in which fractional orders and nonzero intercepts are adjustable parameters are inordinately sensitive to the quality of the data. In our opinion, the closer fit to a one-half order cannot be interpreted beyond simply a demonstration of the general principle.

(35) The values of k_{obsd} are independent of LiHMDS and free hexamethyldisilazane concentrations (zeroth order).

(36) Simple O-alkylations of quinazolinone **5** were problematic. O-Silylation proceeded without event, but desilylation tended to occur under the conditions of the 1,2-addition.

(37) (a) Chadwick, S. T.; Rennels, R. A.; Rutherford, J. L.; Collum, D. B. *J. Am. Chem. Soc.* **2000**, *122*, 8640. (b) Lucht, B. L.; Bernstein, M. P.; Remenar, J. F.; Collum, D. B. *J. Am. Chem. Soc.* **1996**, *118*, 10707.

(38) Trauner and co-workers recently reported a crystal structure of an aryllithium with an ortho methoxymethyl protected phenol in which only the methoxy group coordinates to lithium: Hughes, C. C.; Scharn, D.; Mulzer, J.; Trauner, D. *Org. Lett.* **2002**, *4*, 4109.

(39) Quenching the reaction with aqueous NH₄Cl followed by an extractive workup affords a crude mixture of two compounds displaying spectroscopic behavior consistent with tautomeric imino ethers. Alternatively, quenching the reaction with 2 N HCl affords the dihydroquinazolinone.

(40) The data for the 18 runs used to determine the order in PhCCLi were fit to eq 7 and averaged, affording $\alpha = 1.01 \pm 0.09$.

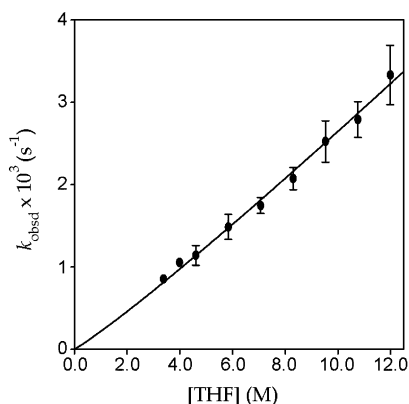


Figure 13. Plot of k_{obsd} versus [THF] in pentane cosolvent for the 1,2-addition of PhCCLi (0.05 N) to **11** (0.005 M) at $-40\text{ }^{\circ}\text{C}$. The curve depicts an unweighted least-squares fit to $k_{\text{obsd}} = a[\text{THF}]^b$ ($a = (2.1 \pm 0.2) \times 10^{-4}$, $b = 1.09 \pm 0.04$).

of nonnucleoside reverse transcriptase inhibitors **2–4**.¹ Using unprotected quinazolinones with consequent in situ formation of lithium salt **8** markedly simplifies the synthesis by avoiding a formal protection–deprotection sequence. The coexistence of five lithiated species, however, introduces potentially enormous structural and mechanistic complexities.^{7–9}

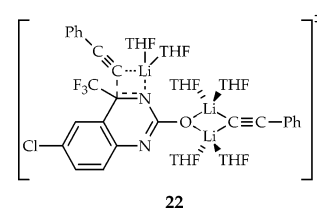
We have taken a step toward understanding the enantioselective addition by investigating the nonenantioselective variant in eq 2. Omission of the amino alkoxide **7** simplified the problem. Even so, the structural control necessary to carry out detailed rate studies required careful planning and an element of luck. We knew that readily purified LiHMDS¹³ could be used in excess as a proton scavenger without the intervention of LiHMDS mixed aggregates.^{9,14,15} The control of the lithium acetylide structure was essential. Although lithium acetylides in THF and THF/hydrocarbon mixtures normally exist as mixtures of cyclic dimers and cubic tetramers, we found that PhCCLi exists as dimer **14** to the exclusion of tetramer **15** in THF and THF/pentane mixtures. The reluctance to form cubic tetramers is unique to this particular lithium acetylide/solvent combination¹⁶ for reasons that are unclear.¹⁸

Characterizing and controlling the structure of lithium quinazolinide salt **8** in the presence of PhCCLi was particularly challenging. At the very low temperatures used to investigate solution structures, a mixture of excess PhCCLi and **8** in THF/pentane solutions affords primarily ladder-based mixed tetramer **16** (or an isomeric ladder) along with low concentrations of mixed dimer **13**. However, the conditions that are optimal for rate studies, low total mixed aggregate concentrations, high THF concentrations, and elevated temperatures, promote the formation of mixed dimer **13**. Consequently, the rate studies were carried out with mixed dimer **13** as the dominant mixed aggregate ($\geq 90\%$; Figure 9), rendering tetramer **16** largely inconsequential.

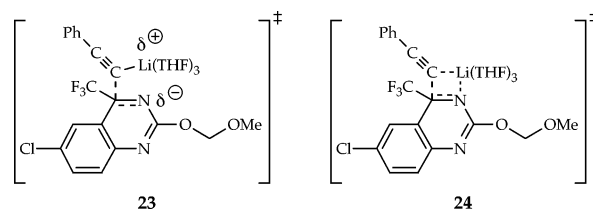
Monitoring the rate of the 1,2-addition by in situ IR spectroscopy and ¹⁹F NMR spectroscopy provided self-consistent results; the high resolution offered by ¹⁹F NMR spectroscopy was particularly convenient.²⁹ Given the complexity of this case study, we took special precautions to show that the reaction was first order in dimer **13**. (A method based on a nonlinear least-squares best fit to eq 7 is noteworthy.) At low THF concentrations wherein tetramer **16** becomes a significant component, deviations from first order are observed. Control

experiments show that LiHMDS and its conjugate acid (HMDS) do not influence the rate. The reaction also appears to be zeroth order in THF, indicating no additional per-lithium solvation of **13** or **14** occurs en route to the rate-limiting transition structure. Finally, an approximate half-order dependence on PhCCLi indicates that PhCCLi dimer **14** dissociates to a disolvated monomer before the 1,2-addition. The collective concentration dependencies are consistent with the idealized rate law and mechanism illustrated in eqs 8–10.

Although, in principle, mixed dimer **13** contains the components necessary for a 1,2-addition, the structural and rate data implicate a transition structure of stoichiometry $[(\text{PhCCLi})_2(\text{8})(\text{THF})_6]^{\ddagger}$ (eq 10).^{41,42} Of course, the rate law does not provide insight into connectivity or the three-dimensional structure. We envision $[(\text{PhCCLi})_2(\text{8})(\text{THF})_6]^{\ddagger}$ as a composite of mixed dimer **13** and PhCCLi(THF)₂ monomer and provide **22** as a working model. The most important implication of this model is that mixed dimer **13** is simply a protected quinazolinone and the PhCCLi component of mixed dimer **13** is of no mechanistic consequence.



We investigated the analogous 1,2-addition to O-protected quinazolinone **11** to understand the nuances of the 1,2-addition to lithium quinazolinide **8**. The methoxymethyl protecting group was chosen due to its ease of preparation;³⁶ mounting evidence argues that the often-cited special (polydentate) ligating properties of acetals are overstated.^{37,38} Quinazolinone **11** is 10^2 – 10^3 times more reactive than mixed dimer **13** toward 1,2-addition, qualitatively consistent with the relative electron densities on **11** and **13**. The first-order dependence on the THF concentration (Figure 13) and the half-order dependence on the PhCCLi concentration are consistent with a trisolvated PhCCLi-monomer-based addition. Conventional thinking might suggest that the three coordinated THF ligands implicate a transition structure such as **23** lacking an N–Li interaction (and the affiliated Lewis acid assistance⁴³) so as not to exceed four-coordinate lithium. One could further argue that this pathway does not appear in the 1,2-addition to mixed dimer **13** due to the excessive electron density that would develop at the transition structure or the steric demands of the mixed dimer coordination sphere.



- (41) Edwards, J. O.; Greene, E. F.; Ross, J. *J. Chem. Educ.* **1968**, *45*, 381.
 (42) Rutherford, J. L.; Hoffmann, D.; Collum, D. B. *J. Am. Chem. Soc.* **2002**, *124*, 264.
 (43) Casado, F.; Pisano, L.; Farriol, M.; Gallardo, I.; Marquet, J.; Melloni, G. *J. Org. Chem.* **2000**, *65*, 322.

Conversely, we believe that the observed trisolvation does not necessarily exclude a Li–N interaction. There is evidence that lithium can exceed four-coordinate.^{44–48} Three poignant examples include: (1) octahedral $+Li(\eta^2\text{-DME})_3$, commonly observed crystallographically;⁴⁴ (2) a trigonal bipyramidal $+Li(\text{THF})_5$ observed crystallographically;⁴⁵ and (3) $(\text{Me}_3\text{Si})_2\text{N}Li(\text{THF})_4$ (and the oxetane-solvated analogue) observed spectroscopically.⁴⁶ Therefore, we submit that a contact ion pair such as **24** is reasonable.^{47,48} In fact, reflecting back on transition structure **22**, it is not altogether obvious that the six THF ligands would necessarily be distributed evenly on the three lithiums as drawn.

Conclusion

The proximity of an electrophilic imine moiety and potentially nucleophilic acetylide fragment in mixed dimer **13** is provocative. It might be tempting to invoke an intraaggregate condensation. Nonetheless, the rate studies lead us to conclude that mixed dimer **13** is simply an O-protected quinazolinone that reacts with an external (additional) disolvated PhCCLi monomer via transition structure **22**. The condensation of PhCCLi is shown to react analogously through a more highly solvated analogue suggested to be **23** or **24**.

In principle, such studies move us closer to understanding how the enantioselective addition in eq 1 occurs. In practice, significant speculation would be premature. We will, however, ask one rhetorical question: If mixed dimer **13** is a protected quinazolinone, is it possible that chiral lithium amino alkoxide **7** converts lithium quinazolinide **8** to a mixed aggregate that is functionally an O-protected form bearing a chiral auxiliary? We suspect that, despite the complexity of the reaction mixture in eq 1, the high enantioselectivity likely derives from a single, compelling control element.

- (44) Bock, H.; Beck, R.; Havlas, Z.; Schoedel, H. *Inorg. Chem.* **1998**, *37*, 5046.
Bock, H.; Havlas, Z.; Gharagozloo-Hubmann, K.; Sievert, M. *Angew. Chem., Int. Ed.* **1999**, *38*, 2240.
(45) Olmstead, M. M.; Power, P. P.; Sigel, G. *Inorg. Chem.* **1986**, *25*, 1027.
(46) Lucht, B. L.; Collum, D. B. *J. Am. Chem. Soc.* **1995**, *117*, 9863.
(47) Depue, J. S.; Collum, D. B. *J. Am. Chem. Soc.* **1988**, *110*, 5524. Ramirez, A.; Lobkovsky, E.; Collum, D. B., unpublished.
(48) Octahedral sodium cation solvated by six THF ligands has been implicated: Jorgensen, W. L.; Chandrasekhar, J. *J. Chem. Phys.* **1982**, *77*, 5080.

Experimental Section

Reagents and Solvents. THF and pentane were vacuum-transferred from degassed blue or purple stills containing sodium benzophenone ketyl. The pentane still contained 1% tetraglyme to dissolve the ketyl. Air- and moisture-sensitive materials were manipulated using vacuum line and syringe techniques. Quinazolinone **5** was prepared using a literature procedure.¹ Quinazolinones $[1\text{-}^{15}\text{N}]\mathbf{5}$ and $[3\text{-}^{15}\text{N}]\mathbf{5}$ were prepared using $[^{15}\text{N}]\text{chloroaniline}$ (>99%) and $[^{15}\text{N}]\text{benzyl isocyanate}$ (99%).¹ $[^6\text{Li}]\text{PhCCLi}$ and $[^6\text{Li},^{13}\text{C}]\text{PhCCLi}$ were prepared in situ using triply recrystallized $[^6\text{Li}]\text{LiHMDS}^{13}$ and commercially available phenylacetylene and $[^{13}\text{C}\text{-}2]\text{phenylacetylene}$. The phenylacetylenes were vacuum-transferred from 4 Å molecular sieves. Lithium salt **8** was generated in situ from quinazolinone **5** and LiHMDS.

NMR Spectroscopic Analyses. All NMR tubes were prepared using stock solutions and sealed under partial vacuum. $[^6\text{Li}]\text{LiHMDS}$ was kept in excess at all times to scavenge the acidic protons of phenylacetylene and quinazolinone. Standard ^6Li , ^{13}C , and ^{19}F NMR spectra were recorded on a 400 MHz spectrometer at 58.84, 100.58, and 376.38 MHz (respectively). The ^6Li , ^{13}C , and ^{19}F resonances are referenced to 0.3 M $[^6\text{Li}]\text{LiCl}/\text{MeOH}$ at -90°C (0.0 ppm), the CH_2O resonance of THF at -110°C (67.35 ppm), and C_6F_6 (-162.55 ppm set at the recording temperature), respectively. The spectra were recorded with a three-channel probe designed to accommodate lithium and carbon pulses. $^6\text{Li},^{13}\text{C}$ -HMQC spectroscopy²¹ and $^1J(^6\text{Li},^{13}\text{C})$ -resolved spectroscopy have been reported.^{9,22–23}

Rate Studies by ^{19}F NMR Spectroscopy. All spectroscopic samples for monitoring the rate of the 1,2-additions were prepared using stock solutions, sealed under partial vacuum, and stored at -78°C (for mixed dimer **13**) or at -196°C (for quinazolinone **11**) before analysis. Detailed protocols are outlined in the Supporting Information.

Acknowledgment. The Cornell group thanks the National Institutes of Health and DuPont Pharmaceuticals for direct support of this work. T.F.B. thanks the National Institutes of Health for a Chemistry-Biology Interface Training Grant (T32-GM08500). The Cornell group also thanks Merck, Pfizer, Boehringer-Ingelheim, R. W. Johnson, Aventis, and Schering-Plough for indirect support.

Supporting Information Available: NMR spectra, rate data, and experimental protocols (PDF). This material is available free of charge via the Internet at <http://pubs.acs.org>.

JA0305813